Investigation on the behavior of the atmospheric dynamics during occurrences of Ozone Hole's Secondary Effect at Southern Brazil

Gabriela Dornelles Bittencourt[1], Damaris Kirsch Pinheiro[1], José Valentin Bageston[2], Hassan Bencherif[3;6], Luis Angelo Steffenel[4], Lucas Vaz Peres[5]

[1] Federal University of Santa Maria, Santa Maria – RS, Brazil
[2] National Institute for Space Research, Southern Regional Space Research Center, Santa Maria – RS, Brazil
[3] University of Reunion Island, LACy, UMR 8105, Reunion, France
[4] Centre de Recherche en STIC, Université de Reims Champagne-Ardenne, Reims, France.
[5] Federal University of Western Pará, Santarém – PA, Brazil
[6] School of Chemistry and Physics, University of KwaZulu-Natal, Westville, Durban, South Africa

Correspondence to: Gabriela Dornelles Bittencourt (gadornellesbittencourt@gmail.com)

Abstract. The Antarctic Ozone Hole (AOH) directly influences the Antarctic region where its levels can reach values below 220 DU. The temporary depletion of ozone in Antarctica generally occurs between the beginning and mid-August, during the austral spring, and extends to November, where a temporary reduction in ozone content is observed in a large region over the Antarctic continent. However, masses of ozone-depleted air can break away from the Ozone Hole and reach middle ltitude regions in a phenomenon known as the Secondary Effect of the Antarctic Ozone Hole. The objective of this paper is to show how atmospheric dynamics behave during the occurrence of this type of event, especially in middle latitude regions, such as southern Brazil, over a 12-year observation period. For the analysis and identification of the events of influence of the AOH on the southern region of Brazil, data from the Total Ozone Column were used from ground-based and satellite experiments, the Brewer Spectrophotometer (MkIII #167) and the Ozone Monitoring Instrument (OMI) on the Aura satellite. For the analysis of the stratospheric and tropospheric fields, the ECMWF reanalysis products were used. Thus, 37 events of influence of the AOH that reached the southern region of Brazil were identified for the study period (2006-2017), where the events showed that in approximately 70% of the cases they occurred after the passage of frontal systems and/or atmospheric blocks over the Southern Brazil. In addition, the statistical analysis showed a strong influence of the jet stream on middle latitude regions during the events. Among the 37 identified events, 92% occurred in the presence of the subtropical and/or polar jet stream over the region of study, possibly explaining the exchange of air masses of ozone deficient in the Upper Troposphere – Lower Stratosphere (UT-LS) region.

1 Introduction

Discovered in 1840 by Christian F. Schonbein, ozone is the most important constituent of stratospheric gas traces which, together with Water Vapor (H_2O) and Carbon Dioxide (CO_2), is responsible for the Earth's energy balance (SEINFELD

35   AND PANDIS, 2016). Due to its ability to absorb ultraviolet radiation (UV) (SALBY, 1996; DOBSON, 1968), O_3 is the most important component in the stratosphere from the point of view of the skin protection against the harmful UVB solar radiation (even considering that a small portion this spectrum can pass through the O_3 layer and hit the ground surface). Most of its atmospheric content (about 90%) is concentrated in the stratosphere between 15 and 35 km altitude (LONDON et al., 1985) in the region known as "ozone layer".

40   The concentration of ozone in a particular region of the Earth is mainly determined by the meridional transport of this element in the stratosphere (GETTELMAN et al., 2011). The explanation for the higher concentration of ozone found in polar rather than equatorial regions (where there is greater production) is precisely a special type of poleward transport known as the Brewer-Dobson circulation, in which air masses are transported quasi-horizontally from the stratospheric tropical reservoir to polar regions (BREWER, 1949; DOBSON, 1968; BENCHERIF et al., 2007 and BENCHERIF et al.,

45   2011). The poleward transport of stratospheric ozone is one of the essential factors for the concentration of this atmospheric constituent in a certain region of the planet (PLOEGER et al., 2012), being much studied from the use of Potential Vorticity, which correlates with the transport of chemical constituents traces such as Ozone (O_3), Nitrous Oxide (N_2O) and Water Vapor (H_2O) on isentropic surfaces in the lower stratosphere. The Potential Vorticity (PV) acts as a dynamical tracer for large-scale air mass transport, behaving as a material surface where the potential temperature is conserved (HOSKINS et al.,

50   1985). In the lower reaches of the stratosphere the lifetime of O_3 molecules is longer and therefore they can be used as a tracer in the study of air mass flow in the Stratosphere-Troposphere Exchange events (BUKIN et al., 2011).

The first studies discussing the ozone concentration on Polar Regions showed that during the spring of the Southern Hemisphere there was a massive reduction of the O_3 content, being known as Antarctica Ozone Hole (AOH) (CHUBACHI et al., 1984; FARMAN et al., 1985 and SOLOMON et al., 1999).The ozone hole area is defined when there is a region with

55   values below 220 DU, less than two thirds of the historical level (HOFMANN et al., 1997). Nevertheless, temporary destruction directly influences ozone content around the Polar Regions due to the crossing of the polar vortex boundary over these regions, causing drastic reductions in the ozone content and increase of the levels of surface ultraviolet radiation (CASICCIA et al., 2008). Studies by Guarnieri et al. (2004) have shown that reductions of up to 1% in total ozone content in southern Brazil cause an average 1.2% increase in surface ultraviolet radiation. In addition, increased ozone-related

60   ultraviolet radiation may also affect aquatic and terrestrial systems, helping to explain the decline in amphibian species associated with genetic malformations caused by increased radiation levels received (SCHUCH et al., 2015). However, their effects can affect regions of mid- and low-latitudes, causing temporary decreases in the total columns of ozone.

Poor ozone air masses are released from the interior of the Antarctic polar vortex, the edge of the Ozone Hole, being carried by the polar filaments on these regions (MARCHAND et al., 2005), in a phenomenon called "Secondary effect of the

65   Antarctic Ozone Hole" causing a temporary fall in ozone content, first observed by Kirchhoff and collaborators (1996) over the South of Brazil. Peres et al., (2014) and Peres et al., (2016) showed the effects of this secondary event on middle latitude

regions such as the southern region of Brazil, where ozone content falls over the region from August to November. Recently, Bittencourt et al. (2018) reported on the second most intense event ever recorded in the southern region of Brazil. According to the latest World Meteorological Organization (WMO) reports (2014 and 2018) there is a growth trend between the 80's and 90's, stabilizing at high rates since the years 2000, despite indications of declining trends in the Antarctic ozone in recent years (SOLOMON et al., 2016).

Unlike other regions of Brazil, the weather conditions in southern Brazil are strongly influenced by transient meteorological systems (REBOITA et al., 2010). Examples of such systems are cold and hot fronts, which carry strong west winds at high tropospheric levels called jet streams. Moreover, the Upper Troposphere – Lower Stratosphere (UT-LS) region in southern Brazil seems to be the home place of many dynamical processes such as stratosphere-troposphere exchanges and isentropic transport between the tropical stratosphere reservoir, polar vortex and mid-latitude. Indeed, understanding the patterns of the UT-LS is important in understanding transport and exchange processes, and the links with tropospheric meteorology (OHRING et al., 2010).

Because of this, the main objective of this paper is to show how atmospheric dynamics behave during the occurrence of events of influence of the Antarctic ozone hole over mid-latitude regions such as southern Brazil, during a 12-year observation period. In addition, recent works (Peres et al., 2014; Bittencourt et al., 2018) show that there is a secondary influence of the ozone hole with these regions where the tropospheric dynamics behavior can influence most cases in the occurrence of these events.

2 Data and Methodology

2.1 Region of Study and Instruments

The region of study was the central portion of Rio Grande do Sul, comprising the city of Santa Maria – RS (29.72°S; 53.72°W). In this work two instruments were used for the analysis of the total ozone content over the southern region of Brazil for a period of 12 years of data (2006-2017). The ground based instrument denominated Brewer Spectrophotometer, (Brewer Model MarK - Brewer MKIII, # 167), now on referred only as Brewer (BREWER MODELS), operated in the municipality of São Martinho da Serra –RS (about 30 km from the city of Santa Maria – RS), and data from OMI instrument were used for the days when there were no Brewer measurements, completing the database for the region of study.

Total Ozone Column (TOC) measurements were obtained by using data from Brewer Model MBIV # 081 spectrophotometers during the period 1992 - 2000; from the model MKII # 056 from 2000 to 2002, and finally by the model MKIII # 167 from 2002 until today. All the above-listed instruments operated at the Southern Space Observatory (SSO), located about 14 km from downtown São Martinho da Serra - RS (29.44°S, 53.82°W, Elev 476 m). The Brewer instrument

operating at SSO/INPE is part of Brewer's Brazilian network that is calibrated against standard travel reference Brewer # 017, managed by International Ozone Services (IOS), and Brewer # 158 from manufacturer Kipp & Zonen (SCI TEC, 1988).

100

Brewer is a fully automated instrument designed for terrestrial measurements of spectral irradiations in the UV-B range of the solar spectrum at five wavelengths, 306.3; 310.1; 313.5; 316.8 and 320.1 nm (KERR et al., 2010), with an approximated resolution of 0.5 nm, allowing to obtain the Total Column of Ozone (O_3) and Sulfur Dioxide (SO_2) (FIOLETOV et al., 2005). The MKIV instrument also measures intensity of radiation in the visible part of the spectrum (430-450nm) and uses

105 differential absorption in this region to infer Total Column Nitrogen Dioxide (BREWER MANUAL). This instrument also permits to obtain the optical thickness of atmospheric aerosols and the vertical O_3 profile by the Umkehr technique (KERR, 2002; and BREWER MANUAL).

Peres et al. (2019) analyzed a long-term (35-year) Total Ozone Column (TOC) series for southern Brazil using Brewer data

110 and satellites, where they showed good agreement between ground-based and satellite instruments. Vanicek (2003) presented a history of calibrations of the Dobson and Brewer instruments in Prague, Czech Republic, where the correct function of the Brewer spectrophotometer was shown and, consequently, its accurate observation process, which depends only on the precise adjustments of the optics as components brewer's electronics and mechanics. In South America, the accuracy and quality of TOC data is ensured by cross calibration using the Brewer # 017 calibrator, allowing a deviation of only about

115 0.58% from daily averages (FIOLETOV et al., 2005).

The Ozone Monitoring Instrument (OMI) was launched on July 2004 onboard the NASA's Earth Observing System Aura satellite (LEVELT et al., 2006) is a continuity of the records made by the Total Ozone Mapping Spectrometer (TOMS) NASA's program that began in 1978 and was officially closed in 2007 (NASA's website). This state of art instrument OMI

120 measures the TOC besides other atmospheric parameters related to ozone chemistry and climate (e.g., NO_2, SO_2). OMI also can distinguish distinct types of aerosols (such as smoke, dust, and sulfates) and measures the atmospheric pressure and cloud coverage. The Earth's atmosphere is observed in 740 spectral bands of wavelength along the satellite path, with a band large enough to provide global coverage in 14 orbits (1day). The 13 x 24 km spatial resolution can be expanded to 13 x 12 km to detect and track sources of pollution on an urban scale, and observes the atmosphere in two ultraviolet bands, named

125 UV-1 (270 to 314 nm) and UV-2 (306 to 380 nm), with a spectral resolution of 0.45 and 1 nm, respectively (LEVELT et al., 2006). In terms of the TOC (in Dobson Unit, DU), the OMI presents an absolute accuracy (the root sum of square of all (1σ) errors) of 3% and a relative accuracy of 1%, respectively for the full vertical column and for the 13 x 24 km in horizontal resolution (LEVELT et al., 2006).

130 We also used reanalysis data available at the Era-Interim/ECMWF, and described by Dee et al. (2011), where meteorological fields were prepared for the analysis of the stratospheric and tropospheric dynamics. Due to radiosonde limitations on the

region of study, the spatial resolution used was 2.5º x 2.5º latitude/longitude, responding well to the objectives of this work, where a higher resolution is not necessary for further details. For the stratospheric dynamics analysis, data of potential vorticity and ozone mixing ratio were used at the potential temperature levels of 265 K and 850 K. For the analysis of tropospheric dynamics it was used winds data (components u, v and w), geopotential height and layer temperature available from 1000hPa to 1 hPa, at the pressure level, in addition to pressure data at mean sea level were used. With these data, potential vorticity fields were made for the potential temperature levels of 600 K and 700 K. For tropospheric fields, sea level pressure and layer thickness between 1000 and 500 hPa, horizontal layer cut showing the jet at 250 hPa and Omega at 500 hPa, and a vertical cut of the layer between 1000 and 50 hPa of potential temperature and wind (m/s) for the longitude of 54ºW.

The HYSPLIT/NOAA model was used to help identifying the events of influence of the Antarctic Ozone Hole over the region of study (ROLPH et al., 2017). The Lagrangian HYSPLIT model is a complete system for calculating simple trajectories of air parcels as well as complex transport simulations, chemical transformation and deposition (HYSPLIT, 2017). The model assumes that a particle follows the wind flow passively its trajectory is the integration of the particle position vector in space and time. In this study, which aims to show the air mass behavior for four days before the events, the HYSPLIT model, an isentropic vertical velocity model, was used to assist in the observation of possible event days over the region, available in HYSPLIT (2017).

2.2 Identification of AOH Influence Events

The identification of the events of influence of the AOH is done first by the analysis of the average daily data of the TOC through instruments on board of satellites and on the ground. In this work, 12 years of satellite data were analyzed with the aim of identifying days where the mean daily value of TOC is less than the climatological average for the month of analysis, i.e., the climatological average minus 1.5 of its standard deviation value ($\mu - 1,5\sigma$), where, μ is a climatological average for the month of interest, σ is the standard deviation, and the value of -1.5 is the criterion chosen from the normal frequency distribution tests (WILKS et al., 2006). This criterion was also used by Peres (2016), where it was observed that the variations around the mean value can represent well the influences of the ozone content in the region of investigation.

After identifying the possible days of influence of the AOH over the region of study, the analysis of isentropic surfaces was conducted, where Absolute Potential Vorticity (APV) fields were made. For the analysis of the stratospheric dynamics, we used reanalysis data available on the Era-Interim/ECMWF platform and the APV fields were analyzed on isentropic surfaces for the potential temperature levels of 600 K and 700 K. Potential Vorticity (PV) was used in previous studies that correlated PV with chemical constituents such as ozone, water vapor and nitrous oxide on isentropic surfaces (adiabatic surfaces where the potential temperature remains constant) in the lower troposphere (SCHOEBERL et al., 1989).

In these case studies, the PV acts as a dynamic large-scale air mass tracer and can be used as a horizontal coordinate (HOSKINS et al., 1985). In this way, this type of analysis aims to verify the origin of the air masses in which an APV increasing is observed when the air mass originates from highest latitudes (e.g., Antarctica). For this analysis, it is needed to consider the previous days of the event or equatorial origin when a decrease of Absolute Potential Vorticity occurs (SEMANE et al., 2006). Bittencourt et al., (2018) and Bresciani et al., (2018) showed the analysis of an extreme event of influence of the AOH on regions of middle latitudes through the analysis of the stratospheric dynamics with the fields of PV.

In the analysis of potential vorticity fields, the air mass trajectory was observed. When there is an increase in the APV it can be stated that the mass of air had polar origin, and other wise (decrease in the APV) the air mass has equatorial origin. As described above, the APV acts as a dynamic marker for large-scale air masses and, thus, observations are made to identify the Secondary Effect of AOH, where reductions in O_3 content are observed from intense to moderate (BITTENCOURT et al., 2018 and PERES et al., 2016).

2.3 Tropospheric Analysis

After identifying all the events for the study period (2006-2017), meteorological fields were prepared for the analysis of tropospheric dynamics, which aims to show how the troposphere behaved before, during and after the occurrence of every event of Secondary Effect of the AOH identified in southern Brazil. Peres et al., (2014) showed a case study of 2012, presenting two events of influence of the AOH on the southern region of Brazil, in which the synoptic analysis was done for the region on the day of the event. The results showed that one of the events occurred just after the passage of a frontal stationary system, where then the arrival of a high pressure system helped to stabilize the region and in the advance of the air masses poor in O_3, configuring the occurrence of the AOH influence event.

The meteorological data for the construction of the pressure fields at Sea level and the layer thickness between 1000 hPa and 500 hPa were obtained by the ECMWF, and the purpose here is to check which synoptic systems were predominating during the events. A presence of the subtropical jet is intended to be displayed in the field of horizontal winds at 250 hPa and Omega at 500 hPa. In addition, ascending and descending surface movements were identified. Another field analyzed was the vertical cut of the atmosphere at different levels of potential temperature (in Kelvin) and wind components (in m/s) for the longitude of 54ºW. In this case, the jet stream was present at higher levels of the troposphere which may aid in air exchanges from the stratosphere to the troposphere (SANTOS, 2016).

2.4 Statistical Analyzes

The average daily data of the ECMWF for the horizontal wind components (zonal- u, and meridional -v) and also the vertical movement velocity (Omega - w) were used for this analysis. In addition, temperature and geopotential height or the available pressure levels between 1000 and 1 hPa, and the component of PV and O_3 for the level of 700 K potential temperature were used. These data were correct read and organized into matrices with the daily averaged values for each of these variables (temperature, u, v and w, geopotential, PV and O_3) in a grid of 2.5° latitude by 2.5° longitude at the levels previously used.

As the set of data used in the preparation of the stratospheric and tropospheric analysis fields was only for the months of interest in this analysis, from August to November in 12 years, the reduction of this dataset allowed the separation of the days of interest (days of occurrence of events of influence of the AOH on the southern region of Brazil), and the subsequent calculation of the monthly averages.

For stratospheric analysis, mean fields of all identified events were made for a period of 3 days before and after each event. For the anomaly analysis of the potential vorticity fields, the following expression was used:

$$\Delta(PV) = PV_{anomaly} = PV_{climatological} - PV_{average(2006\text{-}2017)} \tag{1}$$

Equation 1is used in the following way: the average of all events for each month is used and then this value is decreased, from the month's climatological average.For the tropospheric statistical analyses, the average fields of the identified events of horizontal cut of the atmosphere were made with the objective of analyzing the behavior of the jet stream at 250 hPa and Omega at 500 hPa.

3 Results and Discussion

In this work, the daily average data of the total ozone column were analyzed from the two instruments described above (Brewer and OMI), comprising a 12-year analysis period from 2006 to 2017, mainly from August to November (southern spring). Comparing the two instruments (Figure not shown here, but very similar to Figure 2 of Peres et al., 2019), the correlation index found here considered very high, i.e. $R^2 = 0.96$, showing high proportionality between the instruments used in this study. The results are also similar to the observations reported by Antón et al. (2009) for the Iberian Peninsula, where the Brewer and OMI total ozone datasets were compared and also with other results from separate ozone monitoring stations around the world (HENDRICK et al., 2011; KECKHUT et al., 2010).

After the identification of the mean daily data of the TOC and analysis of the monthly climatology of the data observed at SSO, the first step for the identification of AOH side effect events over the study region is the analysis of the climatological average for the reference months and the occurrence of AOH during the extended austral spring period (August to

November). For this, days are chosen in which strong decreasing in the ozone content is observed, i.e., when the average daily value of the total ozone column is less than the average climatological value (for the respective month) minus 1.5 of its standard deviation (μ–1,5σ). Table 1 shows the TOC monthly climatological values with monthly standard-deviation, together with the lower TOC limit, for the extended spring season.

After the confinement of the drop limits presented in Table 1, we analyzed 90 days where the TOC value of the respective day was lower than this limit minus 1,5σ. From these days, using a methodology described above, a total of 37 events were identified as important events that reached the southern region of Brazil from August to November in the years from 2006 to 2017. As expected, based on previous works and climatology, the identified events occurred mostly during October, and it is in good agreement with the results found by Peres (2016). To exemplify the analysis developed in this paper, we present in the next section a case study that took place on September 18, 2017, as this is the most recent event identified throughout the observed period, showing a side effect event of AOH in the region of South Brazil. Other interesting, and even more prominent, events have already been reported by Bresciani et al., (2018) and Bittencourt et al., (2018).

3.1 Case Study: Event Observed on September 18, 2017

The event that occurred on 18 Sept. 2017 presented a TOC value, measured by the Brewer Spectrophotometer, of 271.5 DU, representing a decrease of approximately 8.5% in comparison with the climatological average for the month of September, as reported in Table 1. The observed decrease in TOC could be attributed to isentropic transport in the stratosphere.

Figure 1 show the PV fields obtained from ECMWF data at 600K and 700K isentropic levels in the stratosphere. One can see from Figure 1 that Chile, Argentina, Uruguay, South of Brazil and Paraguay are under the influence of the passage of stratospheric air masses characterized by APV values greater than 100. We obtained almost the same PV pattern at the 600K isentropic level. As explained above, PV is a conservative dynamical parameter and indicates the transport of air masses which takes place on isentropic surfaces (HOSKINS et al., 1985). Therefore, PV distributions could be used to determine the origin of air masses. Since PV values are positive in the north hemisphere and negative in the south hemisphere, for convenience, we refer here after to the APV, which is positive regardless of the latitude. From Figure 1 we can observe that PV values are higher than 100 and can be associated to air masses of polar origin, what suggests that the observed decrease in the total ozone column at SSO, in South of Brazil, is a result of the transport of air masses with low ozone concentration from high southern latitudes. In order to corroborate this hypothesis, the Lagrangian HYSPLIT model was initialized on September 18, 2018 at SSO location and run for back-trajectory retrievals in the lower stratosphere (see Figure 2.a). All the stratospheric back-trajectories show that air masses observed over SSO in the South of Brazil travelled northward and eastward over the polar region. This confirms the polar origin of the observed air masses. Moreover, Figure 2.b illustrates the global distribution of TOC recorded by OMI experiment on September 18, 2018. It shows that transport of polar air is

characterized by reduction in TOC distribution extending from the polar region up to mid-latitude region. This well illustrates the side effect of AOH, resulting in a decrease in stratospheric ozone concentrations during the analyzed event.

270

After the identification of the secondary effect of the AOH on the southern region of Brazil on September 18, 2018, the tropospheric dynamics analysis, to observe how the troposphere was behaving during the occurrence of this event. Figure 3 presents the atmospheric fields used in this work for the study of tropospheric dynamics. This type of analysis was used by Bittencourt et al., 2018, where the study was done only for an extreme event of influence of AOH. In the days leading up to
275 the confirmation of the side effect event, the region remained unstable from September 11, 2018 until one day before the event, which can be explained by the isentropic tapering corresponding to a more compressed layer thickness, besides the presence of an intense temperature gradient. For the day of the event September 18, 2018, was observed in the region the formation of a system of high pressure, which moved to the ocean in the following days. Under these circumstances, on the surface, we have a post-frontal high-pressure system near the region of interest, which may have helped to carry this O_3 air
280 mass to reach mid-latitude regions such as central southern Brazil.

The horizontal wind and temperature fields (Figure 3.c and 3.d) show the jet at 250 hPa and the omega at 500 hPa, where the objective here is to identify the regions of upward and downward movement of air masses. The presence of the polar jet in southern Brazil, Argentina and Uruguay is observed in Figures 3.c and 3.d. Negative Omega values at 500 hPa persist
285 throughout the period, indicating upward movement at lower levels of the atmosphere. Thus, the horizontal section of the atmosphere showed that the presence of the polar jet dominates the region until the day of the event confirmation. For this reason, the arrival of O_3 poor air masses in the region may be associated with the performance of a frontal system that passed through the region days before the event was confirmed, as well as the presence of the jet at higher atmospheric levels, helping in the exchanges air from the stratosphere to the troposphere contributing to a temporary reduction in O_3 content on
290 September 18, 2018. The vertical section of the atmosphere between 1000 and 10 hPa of potential temperature and wind at 54° longitude, Figures 3.e and 3.f shows the presence of polar jet current at higher levels of the atmosphere, as well as the isentropic funnel near longitude. from 30°S to September 17, 2018, indicating a frontal ramp, which helps in the air exchange from the highest to the lowest levels on the day of the event.

295 **3.2 Statistical analyses: atmospheric dynamics**

Figure 4 shows the mean field of the 37 AOH influence events identified in this work, where potential vorticity fields were used for the 700 K isentropic level, for three days before and up to three days after the event. Analyzing Figure 4a and 4b, it can be observed that for -3 days (-3d) the variation of potential vorticity over the region remains stable, without variation in
300 the content of APV on the south of Brazil, with APV values between 40 and 60PVU.

Already from 2-days before (-2d) the event, Figure 4.c, we can observe a slight increase in APV values over the study region, mainly between Argentina, Uruguay and Southern Brazil with APV values from 60 to 80 PVU. From one day before (-1d) the event, the increase of APV over the study region becomes more important, with APV values between 100 and 140 PVU. For the days after the event, +1d (Figure 4.e) and +2d (Figure 4.f), air masses with APV higher than 100 PVU bound mid-latitude region in Chile, Argentina, Uruguay and Southern Brazil, with values up to 160 PVU. From the third day after the event, we found a decrease in APV values similar to the -2d situation (not shown). These results indicate that during the 37 identified secondary effect events due to the AOH development, low-ozone air masses are transported from polar region to mid-latitudes and covering a wide region over North of Chile, Argentina, Uruguay and Southern Brazil. In average, such low-ozone event may last and affect that sub-region during at least 4 days. This is agreement with previous works published by Peres (2016).

Plots on Figure 5 show the average monthly distributions of potential vorticity anomalies on the 700 K isentropic level, averaged for August, September, October and November over the study period, 2006-2017. The PV anomaly fields show the predominance of positive potential vorticity anomalies in southern Brazil (values around 35 to 55 PVU). Figure 5.a shows that in August there is a predominance of positive anomalies in southern Brazil, according to the number of events identified this month (7 events, see Table 2) in southern Brazil. November has the lowest number of low-ozone AOH events identified in the region (5 events, see Table 2) and also shows the predominance of a positive anomaly in southern Brazil, with possible vorticity anomalies between 10 and 30 PVU. For the months of September and October, positive PV anomalies were very evident in the 12 years of data.

Significant increases in positive anomalies (between 10 and 50 PVU for September, and from 30 to 60 PVU) are concomitant and consistent with the large number of low-ozone AOH events recorded during these months (12 events in September and 13 events in October). Physically, it is possible to confirm the importance of these months for the analysis, due to the greater number of AOH influencing events that affect southern Brazil, as observed by Bittencourt et al., 2018, which is explained by polar filaments that release from the Ozone Hole region and then bring O_3 to mid-latitude regions.

For a better understanding of the tropospheric dynamics during the 37 events identified, medium fields were made for the horizontal and vertical cuts of the atmosphere. Figure 6 shows the average field for the horizontal cut (jet at 250 hPa and Omega at 500 hPa). In the mean of the 37 AOH influence events identified in this study (Table 2), the presence of the jet stream (subtropical or polar) is observed in practically all identified events, Figure 6 confirms this where the presence of the jet stream is observed mainly on the southern region of Brazil. However, there is a predominance of a center with negative values of Omega at 500 hPa, indicating surface convergence, which explains the majority of events identified after the passage of frontal systems over the southern region of Brazil. Therefore, the importance of the jet stream for the vertical

335 distribution of O_3 in the atmosphere, and also in air exchanges from the stratosphere to the troposphere (BUKIN et al., 2011; SANTOS, 2016) on the southern region of Brazil.

Finally, Figure 7 presents the average for the 37 AOH influence events identified on the Southern Brazil of the vertical cut of the atmosphere between 1000 and 30 hPa. Similar to Figure 6, the presence of the jet stream with an intense nucleus (~ 45 to

340 50 m/s) near the latitude and longitude of the study region, besides the presence of a jet near 30 hPa, indicating the probable presence of the polar jet current in the average of the events. However, it is confirmed that the jet stream (subtropical and / or polar, depending on the case) was also present at higher levels of the atmosphere. Therefore, analyzing the average tropospheric dynamics of the 37 events of influence of the AOH on the southern region of Brazil, the presence of the polar jet stream, at higher levels of the atmosphere, as well as the presence of the subtropical jet stream probably explaining the

345 transport of O_3-poor air masses from polar regions to mid-latitude regions, like the southern Brazil.

4 Conclusions

In this work, we analyzed daily TOC measured by the Brewer Spectrophotometer operational at the SSO site in the South of Brazil, and by OMI instrument from 2006 to 2017. Analysis of TOC datasets revealed 37 low-ozone events that have occurred and extended during the austral spring period (August-September-October-November) over the SSO site.

350 Moreover, examination of potential vorticity fields in the stratosphere (on the 700 K isentropic level) and of back-trajectories obtained by the Lagrangian HYSPLIT model showed that the 37 low-ozone events resulted from the transport of air masses from polar regions to mid-latitudes, and correspond therefore to the secondary effect of the AOH. In addition, it has been shown from PV anomaly fields that the detected events have spread over a large region, covering northern Chile, Argentina, Uruguay and southern Brazil, and can last and affect this sub region for at least 4 days. In accordance with the period of

355 development of the (AOH) and with previous published works, we found that most of the events took place in September (35%) and October (39%), while 17.6% of them were identified in August and 12.7% in November.

The analysis of tropospheric dynamics confirmed the importance of jet as the main synoptic system that assists in the exchange of air masses between the stratosphere and the troposphere. Of the 37 events, about 92% of the cases identified the

360 presence of the jet stream (subtropical and/or polar), in the remaining 8% no action of the jet stream was identified, or it was weak, not assisting in the exchange of air masses. In addition, on the surface, events were identified in 70% of cases after the passage of frontal systems in southern Brazil, where together with the performance of a high-pressure system characterized by downward stabilization of the atmosphere, explains the arrival of ozone-depleting air masses from the Antarctic region that can reach the mid-latitude regions. Regarding the statistical analyzes of the tropospheric fields, confirmation of the

365 importance of the jet stream was obtained. The vertical cut of the atmosphere showed the presence of the two jet streams (polar and subtropical jet) at higher levels of the atmosphere, besides the current lines converge to regions close to 30ºS,

southern region of Brazil. The average fields of the 37 events identified in the region, show the presence of the jet stream in relation to the horizontal cut (jet 250 hPa) and vertical cut (1000 and 30 hPa).

370 The results found here highlight the importance of the jet stream actuation as the main synoptic system that supports the exchange of masses of ozone-deficient air from the stratosphere to the troposphere. It is evident that the two jet streams (subtropical and polar) act together in this exchange mechanism, possibly becoming a "connection" between the two atmospheric layers during the occurrence of events of side effect of the (AOH) on the southern region of Brazil.

375

Acknowledgements. This work is part of the Graduate Program in Meteorology of the Federal University of Santa Maria (UFSM) in cooperation with the Regional Center Space Research (CRS) and National Institute of Space Research (MCTIC/INPE), supported by the Coordination of Improvement of Higher Education Personnel (CAPES). The authors would like to express their thanks to CAPES/COFECUB Program, process nº 88887.130176/2017-01, and National Institute
380 of Antarctic Science and Technology for Environmental Research, CNPq process n° 574018/2008-5 and FAPERJ process n° E-16/170.023/2008, for the financial support. The authors also thank the data provided by NASA (OMI), ECMWF/Era - Interim for daily average data.

385 **References**

ANTÓN, M., LÓPEZ, M., VILAPLANA, J. M., KROON, M., MCPETERS, R.,BAÑÓN, M., AND SERRANO, A.: Validation of OMI-TOMS and OMI-DOAS total ozone column using five Brewer spectroradiometers at the Iberian Peninsula, **J. Geophys. Res.-Atmos**., 114, D14307,doi:10.1029/2009JD012003, 2009.

BENCHERIF H., T. PORTAFAIX, J.L. BARAY, B. MOREL, S. BALDY, J. LEVEAU, A. HAUCHECORNE, P.
390 KECKHUT, A. MOORGAWA, M.M. MICHAELIS, R. DIAB, LIDAR observations of lower stratospheric aerosols over South Africa linked to large scale transport across the southern subtropical barrier, **Journal of Atmospheric and Solar-Terrestrial Physics** 65, 2003.

BENCHERIF H., L. EL AMRAOUI, N. SEMANE, S. MASSART, D.V. CHARYULU, A. HAUCHECORNE AND V. H. PEUCH, Examination of the 2002 major warming in the southern hemisphere using ground-based and Odin/SMR
395 assimilated data: stratospheric ozone distributions and tropic/mid-latitude exchange, **Can. J. Phys**., 85, 1287-1300, 2007

BITTENCOURT, G. D., BRESCIANI, C., BAGESTON, J. V., PINHEIRO, D. K., SCHUCH, N. J., BENCHERIF, H., LEME, N. P., AND PEREZ, L. V.: A Major Event of Antarctic Ozone Hole Influence in the Southern Brazil in October 2016: An Analysis of Tropospheric and Stratospheric Dynamics, **Annales Geophysicae**, 2018

BRESCIANI, C., BITTENCOURT, D. G., BAGESTON, V. J., PINHEIRO, K. D., BENCHERIF, H., SCHUCH, J. N.,
400   LEME, N. P., PERES, V. L., Report of a Large Depletion in the Ozone Layer over the South Brazil and Uruguay by Using Multi – Instrumental Data, **Annales Geophysicae.**, 2018.

BREWER, A. W. Evidence for a world circulation provided by the measurements of helium and water vapor distribution in the stratosphere, **Q. J. R. Meteorol. Soc**., v.75, p. 351-363,1949.

BREWER MODELS., http://kippzonen-brewer.com/about-brewer/history-brewer/.

405   BREWER Website., https://www.esrl.noaa.gov/gmd/grad/neubrew/MkIV.jsp.

BREWER   MANUAL.,   http://kippzonen-brewer.com/wp-content/uploads/2014/10/KippZonen_Operators_Manual_Brewer_MKIII_V1206-1.pdf.

BUKIN, O. A., SUAN An, N.; PAVLOV, A. N.; STOLYARCHUK, S. Y. and SHMIRKO, K .A. Effect that Jet Streams Have on the Vertical Ozone Distribution and Characteristics of Tropopause Inversion Layer, **Iz. Atmos. and Ocean. Phys.**
410   v. 47, n. 5, p. 610–618, 2011.

CASICCIA, C.; ZAMORANO, F.; HERNANDEZ, A. Erythemal irradiance at the Magellan's region and Antarctic ozone hole 1999-2005. **Atmosphere**, v. 21 n.1, p. 1-12, 2008.

CHUBACHI, S. Preliminary result of ozone observations at Syowa Station from February, 1982 to January, 1983. **Mem. Natl. Inst. Polar Res. Jpn. Spec.**, v. 34, p. 13-20, 1984.

415   DEE, D. P., UPPALA, S. M., SIMMONS, A. J., BERRISFORD, P., POLI, P., KOBAYASHI, S., ANDRAE, U., BALMASEDA, M. A., BALSAMO, G., BAUER, P., BECHTOLD, P., VAN DE BERG L, BIDLOT J, BORMANN N, DELSOL C, DRAGANI R, FUENTES M,. The ERA-Interim reanalysis: configuration and performance of the data assimilation system. **Q. J. R. Meteorol. Soc.** 137: 553–597. DOI:10.1002/qj.828, 2011.

DOBSON, G. M. B. **Observations of the amount of ozone in the earth's atmosphere and its relation to other**
420   **geophysical conditions**. Proceedings of the Royal Society of London A, v. 129, n. 411, 1930.

DOBSON, G. M. B., Forty years' research on atmospheric ozone at Oxford: A history. **Appl. Opt**., v. 7, p. 387-405, 1968.

ECMWF/ERA-INTERIM, Daily, **http://apps.ecmwf.int/datasets/data/interim-full-daily/levtype=sfc**, 2017.

FARMAN, J. C.; GARDINER, B. G.; SHANKLIN, J. D. Large losses of total ozone in Antarctica reveal seasonal ClOx/NOx interaction. **Nature**. 315: 207-210, 1985.

425 FIOLETOV, V. E., KERR, J. B., MCELROY, C. T., WARDLE, D. I., SAVASTIOUK,V., and GRAJNAR, T. S.: The Brewer reference triad, **Geophys. Res.Lett.,** 32, L20805, doi:10.1029/2005GL024244, 2005.

GETTELMAN, A., HOOR, P.; PAN, L. L., RANDEL, W. J., HEGGLIN, M. I., BIRNER, T.The Extratropical Upper Troposphere and Lower Stratosphere.**Rev. Geophys.**, v. 49, n. RG3003, 2011.

HENDRICK, F., POMMEREAU, J.-P., GOUTAIL, F., EVANS, R. D., IONOV,D., PAZMINO, A., KYRÖ, E., HELD, G.,
430 ERIKSEN, P., DOROKHOV, V.,GIL, M., AND VAN ROOZENDAEL, M.: NDACC/SAOZ UV-visible total ozone measurements: improved retrieval and comparison with correlative ground-based and satellite observations, Atmos.Chem. Phys., 11, 5975–5995, doi:10.5194/acp-11-5975-2011, 2011.

HOFMANN, D. J., OLTMANS, S. J., HARRIS, J. M., JOHNSON, B. J., LATHROP, J. A. Ten years of ozone sondemeasurements at the South Pole: Implications for recovery of springtime Antarctic ozone. **J. Geophys. Res-Atmos.**,
435 v.102,p.8931-8943, 1997.

HOSKINS, B. J.; McINTYRE, M. E.; ROBERTSON, A. W. On the use and significance of isentropic potential vorticity maps. **Q. J. Roy. Metror. Soc.**, v. 111, p. 877-946, 1985.

KECKHUT, P., HAUCHECORNE, A., BLANOT, L., HOCKE, K., GODIN-BEEKMANN, S., BERTAUX, J.-L., BARROT, G., KYRÖLÄ, E., VAN GI-JSEL, J. A. E., AND PAZMINO, A.: Mid-latitude ozone monitoringwith the
440 GOMOS-ENVISAT experiment version 5: the noise is-sue, Atmos. Chem. Phys., 10, 11839–11849, doi:10.5194/acp-10-11839-2010, 2010.

KERR, J. B.: New methodology for deriving total ozone and other atmospheric variables from Brewer spectrometer direct Sun spec-tra, J. Geophys. Res., 107, 4731, doi:10.1029/2001JD001227,2002.

KIRCHHOFF, V. W. J. H., SCHUCH, N. J., PINHEIRO, D. K., HARRIS, J. M. Evidence for an ozone hole perturbation
445 at30º south. **Atmos. Environ.**, v. 33, n. 9, p. 1481-1488, 1996.

LEVELT, P.., OORD, G.H.J., DOBBER, MARCEL., MÄLKKI, ANSSI., VISSER, HUIB., VRIES, JOHAN., STAMMES, PIET., LUNDELL, JENS, and SAARI, HEIKKI. The Ozone Monitoring Instrument. IEEE T. Geoscience and Remote Sensing. 44. 1093-1101. 10.1109/TGRS.2006.872333, 2006.

LONDON, J. Observed distribution of atmospheric ozone and its variations. In: Whitten, R. C.; Prasad, S. S. ed. **O. in the F.**
Atmos. New York: Van Nostrand Reinhold. cap. 1, p. 11 – 80. 1985.

MARCHAND, M.; BEKKI, S.; PAZMINO, A.; LEFÈVRE, F.; GODIN-BEEKMANN, S.; HAUCHECORNE, A. Model simulations of the impact of the 2002 Antarctic ozone hole on midlatitudes. **J. Atmos. Sci.**, v. 62, p. 871–884, 2005.

NASA Website., https://www.nasa.gov/centers/goddard/news/topstory/2007/toms_end.html.

OHRING, G.; BOJKOV, R. D.; BOLLE, H. J, HUDSON, R. D. and VOLKERT, H. Radiation and Ozone: Catalysts for Advancing International Atmospheric Science Programs for over half a century. **Sp. Res.Today**, n177, 2010.

OMI-ERS2/NASA: AURA Validation Data Center, **https://avdc.gsfc.nasa.gov/index.php?site=1593048672&id=28**, 2018.

PEIXOTO, J. P.; OORT, A. H. **Physics of climate**. New York: Springer, 1992.

PLOEGER, F.; KONOPKA, P.; MUELLER, R.; FUEGLISTALER, S.; SCHMIDT, T.; MANNERS, J. C.; GROOSS, J. U.; GUENTHER, G.; FORSTER, P. M.; RIESE, M. **Horizontal transport affecting trace gas seasonality in the Tropical Tropopause Layer (TTL)**. J. Geophys. Res-Atmos., v. 117, n. D09303, 2012.

PERES, L. V.; REIS, N. C. S. dos.; SANTOS, L. O.; BITTENCOURT, G. D.; SCHUCH, A. P.; ANABOR, V ; PINHEIRO, D. K.; SCHUCH, N. J.; LEME, N. M. P. Atmospheric Analysis of the Events of Secondary Effect of the Antarctic Ozone Hole on Southern Brazil in 2012. Part 2: Synoptic Verification of the Troposphere during the events. SCIENCE AND NATURE. v. 36, p. 423-433, 2014.

PERES, V. L. Monitoring of the total ozone column and the occurrence of events of influence of the Antarctic Ozone Hole over the South of Brazil. **Doctoral thesis**, 2016.

PERES, L. V., BENCHERIF, H., MBATHA, N., SCHUCH, A.P., TOIHIR, A. M., BÈGUE, N., PORTAFAIX, T., ANABOR, V., PINHEIRO, D. K, LEME, N. M.P., BAGESTON, J. V., SCHUCH, N. J. Measurements of the total ozone column using a Brewer spectrophotometer and TOMS and OMI satellite instruments over the Southern Space Observatory in Brazil, **Ann. Geophys.**, 35, 25-37, doi:10.5194/angeo-35-25-2017, 2017.

PERES, LUCAS VAZ; PINHEIRO, DAMARIS KIRSCH; STEFFENEL, LUIZ ANGELO; MENDES, DAVID; BAGESTON, JOSÉ VALENTIN; **BITTENCOURT, GABRIELA DORNELLES** ; SCHUCH, ANDRÉ PASSÁGLIA; ANABOR, VAGNER; LEME, NEUSA MARIA PAES; SCHUCH, NELSON JORGE; BENCHERIF, HASSAN. Long-term

Monitoring and Climatology of Stratospheric Fields when Antarctic Ozone Hole Influence Events Occur in Southern Brazil. **Brazilian Journal of Meteorology**, v. 34, p. 151-163, 2019.

REBOITA, M. S.; GAN, M. A.; ROCHA, R. P.; AMBRIZZI, T. Regimes of precipitation in South America: A Bibliographical Review. **B. J. of Met.**, v. 25, n. 2, p. 185–204, 2010.

ROLPH, G., STEIN, A., AND STUNDER, B. Real-time Environmental Applications and Display sYstem: READY. **Env. M.& Soft.**, 95, 210-228,https://doi.org/10.1016/j.envsoft.2017.06.025, 2017.

SALBY, M. L. **Fund. Atmos.Phys**. International geophysics series, v. 61, Academic Press, 1996.

SANTOS, L. O. Stratosphere Exchange - Troposphere and its Influence on Ozone Content in the Central Region of Rio Grande do Sul. **Master's Dissertation**, 2016.

SEINFELD, J. H.; PANDIS, S. N. **Atmos. Chem. Phys.: From Air Pollution to Climate Change**, Third Edition, John Wiley and Sons, Inc. 2016.

SEMANE, N.; BENCHERIF, H.; MOREL, B.; HAUCHECORNE, A.; DIAB, R. D. An unusual stratospheric ozone decrease in Southern Hemisphere subtropics linked to isentropic air-mass transport as observed over Irene (25.5º S, 28.1º E) in mid-May 2002. **Atmos. Chem. Phys.**, v. 6, p. 1927-1936, 2006.

SCHUCH, P. A., SANTOS, M. B., LIPINSKI, V. M., PERES, L. V, SAN-TOS C. P., CECHIN S. Z., SCHUCH, N. J., PINHEIRO, D. K., AND LORETO, E. L. S.: Identification of influential events concerning the Antarctic ozone hole over southern Brazil and the biological effects induced by UVB and UVA radiation in an endemic tree frog species, Ecotox. Environ. Safe., 118, 190–198,doi:10.1016/j.ecoenv.2015.04.029, 2015.

SCI TEC: Brewer ozone spectrophotometer, Acceptance manual, Doc. AM-BA-C05-Rev C, SCI TEC Instruments, Seoul, 1988.

SCHOEBERL, M. R. Reconstruction of the constituent distribution and trends in the Antarctic polar vortex from ER-2 flight observations**, J. Geophys. Res.**, v.94, p.16.815– 16.845, 1989.

SOLOMON, S. **Stratospheric ozone depletion: A review of concepts and history**. Reviews of Geophysics, v. 37, n. 3, p. 275–316, 1999.

505 SOLOMON, S, IVY, D. J, KINNISON, D., MILLS M. J., NEELY, R. R., SCHMIDT A. **Emergence of healing in the Antarctic ozone layer**, Science, 353(6296), 269-74. DOI: 10.1126/science.aae0061, 2016.

VANICEK, K.: Calibration history of the ozone spectrophotometers operated at the Solar and Ozone Observatory of CHMI in Hradec Kralove, Czech Republic. Publication of the Czech Hydrometeorological Institute, ISBN 80-86690-08-3, Prague, 510 2003.

WMO. World Meteorological Organization: **Scientific Assessmentof Ozone Depletion**. Estados Unidos da América,1996.

WMO. World MeteorologicalOrganization: **ScientificAssessmentof Ozone Depletion**. Estados Unidos da América, 2014.
515
WMO. World MeteorologicalOrganization: **Scientific Assessmentof Ozone Depletion**. Estados Unidos da América, 2018.

520

525

530

535

540

545

Month	Climatology O_3 in DU (μ)	Standard Deviation in DU (σ)	Limit -1,5σ in DU (μ-1,5σ)
August	283.7	12.9	264.3
September	290.7	10.1	275.5
October	284.4	7.2	273.6
November	281.3	9.7	266.7

550

Table 1: Monthly climatological values, their standard deviations and limit -1.5σ for August, September, October and November for the South Space Observatory (SSO).

555

Event Day	O_3Reduction	Event Day	O_3Reduction	Event Day	O_3Reduction	Event Day	O_3Reduction
08/07/2006	11.9 %	**10/26/2008**	6.3 %	**09/14/2012**	8 %	**08/25/2016**	11 %
08/23/2006	9.2 %	**11/01/2008**	10.4 %	**09/22/2012**	4.5 %	**09/05/2016**	8.6 %
09/19/2006	8.7 %	**09/03/2009**	12.9 %	**10/14/2012**	11 %	**09/12/2016**	7.5 %
10/07/2006	8.3 %	**09/29/2009**	7 %	**10/23/2013**	12.3 %	**10/20/2016**	22 %
10/15/2006	7.6 %	**08/08/2010**	5 %	**08/10/2014**	5.4 %	**08/26/2017**	13 %
11/17/2006	11.7 %	**09/08/2010**	4.4 %	**08/22/2014**	10.1 %	**09/18/2017**	8.6 %
09/13/2007	5.4 %	**10/13/2010**	4.6 %	**10/13/2014**	4.2 %	**11/16/2017**	9.5 %
10/07/2007	8.5 %	**10/22/2010**	8.6 %	**11/03/2014**	4 %		
09/28/2008	5.3 %	**10/01/2011**	4.2 %	**09/22/2015**	6 %		
10/12/2008	7 %	**10/21/2011**	4 %	**11/03/2015**	8.5 %		

560   Table 2: Events of Secondary Effect of the Antarctic Ozone Hole over southern Brazil from 2006 to 2017. Average daily TOC value, percentage of O_3 reduction with respect to the climatological average of the month.

565

570
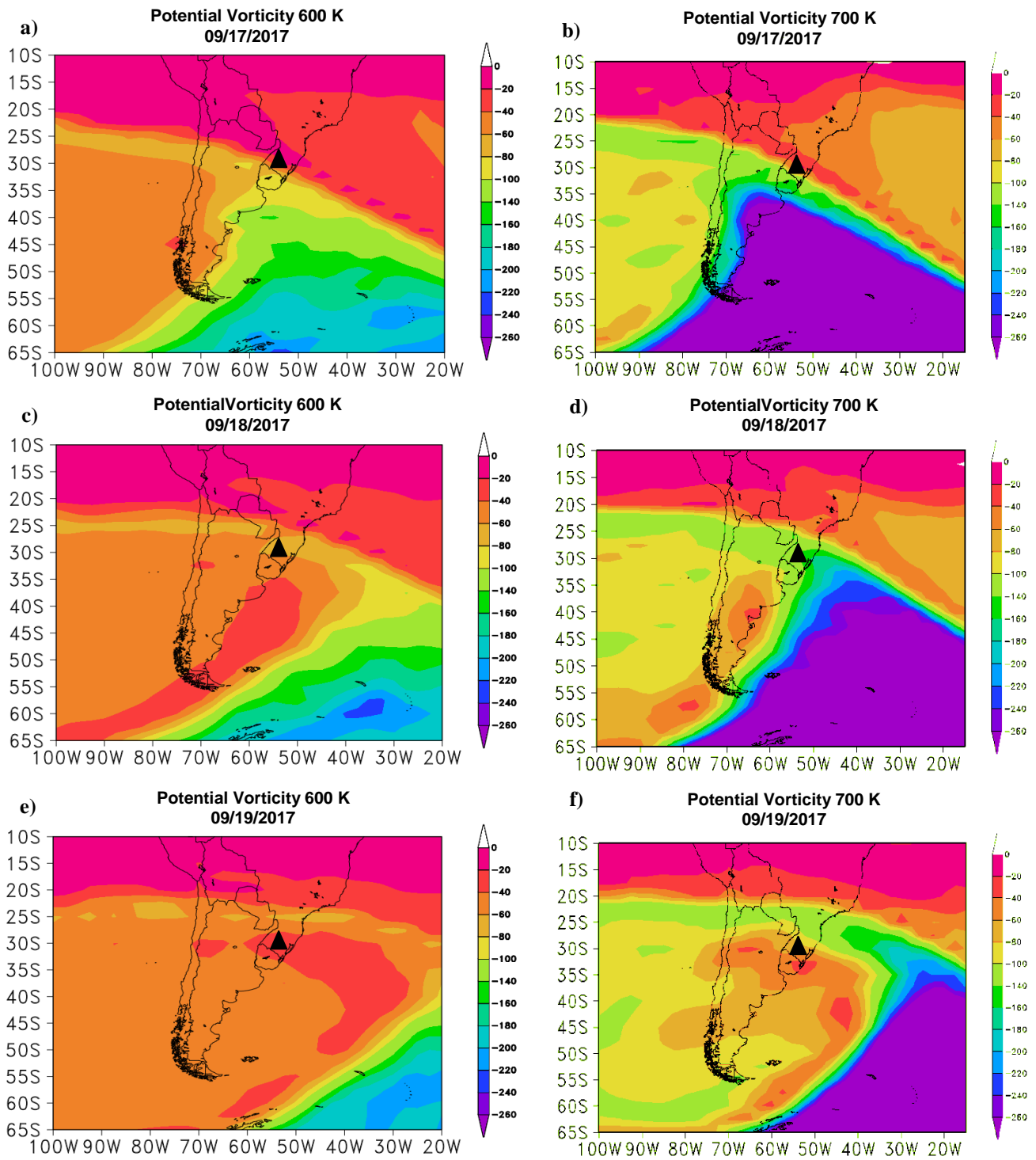
Figure 1: Potential Vorticity fields at the 600 K and 700K isentropic level as derived from ECMWF data successively on (a) and (b) 17 SEPT., (c) and (d) 18 SEPT., and (e) and (f) 19 SEPT. 2017. The black symbol indicates the location of the SSO.

580
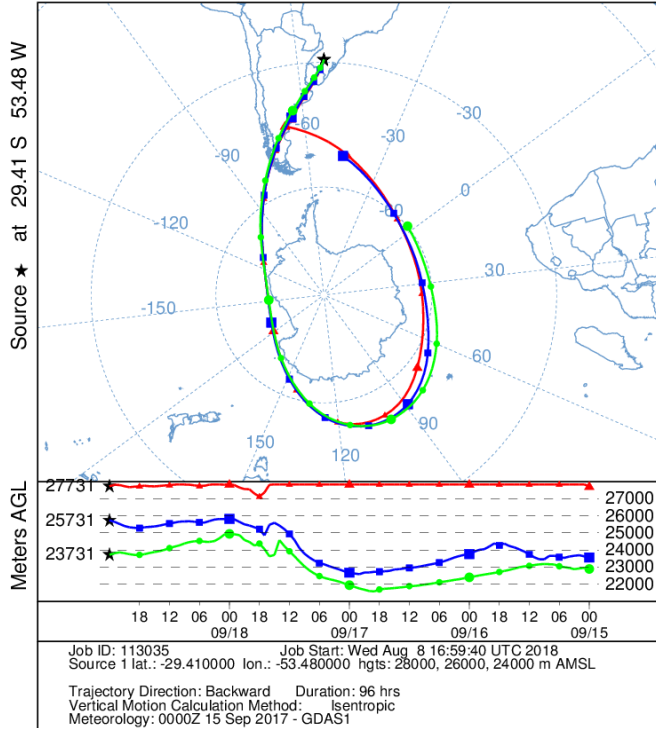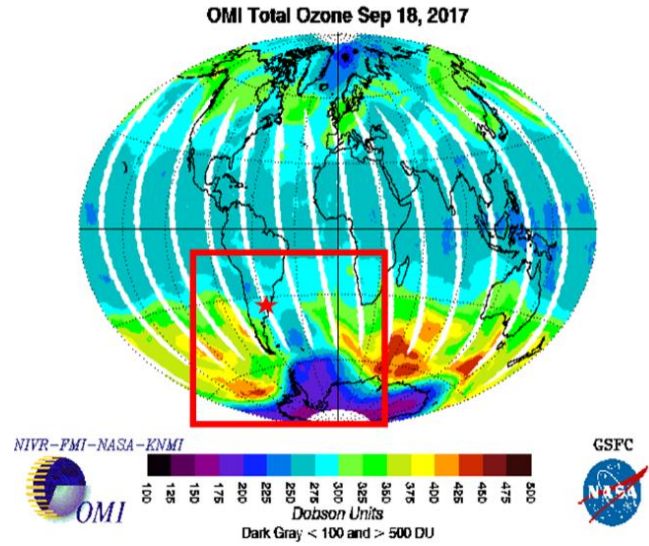
Figure 2: a) Retroactive trajectories as retrieved by model Lagrangian HYSPLIT model, initialized on 09/19/17 00UTC at SSO location. The back-trajectories were run at 20 km (in red), 24 km (in blue) and 28 km (in green) above ground level; b) global TOC distribution as recorded by OMI experiment on 18 SEPT. 2017. The red box focus on the low-ozone event and the stare symbol indicates the location of the SSO site.

590

595

600
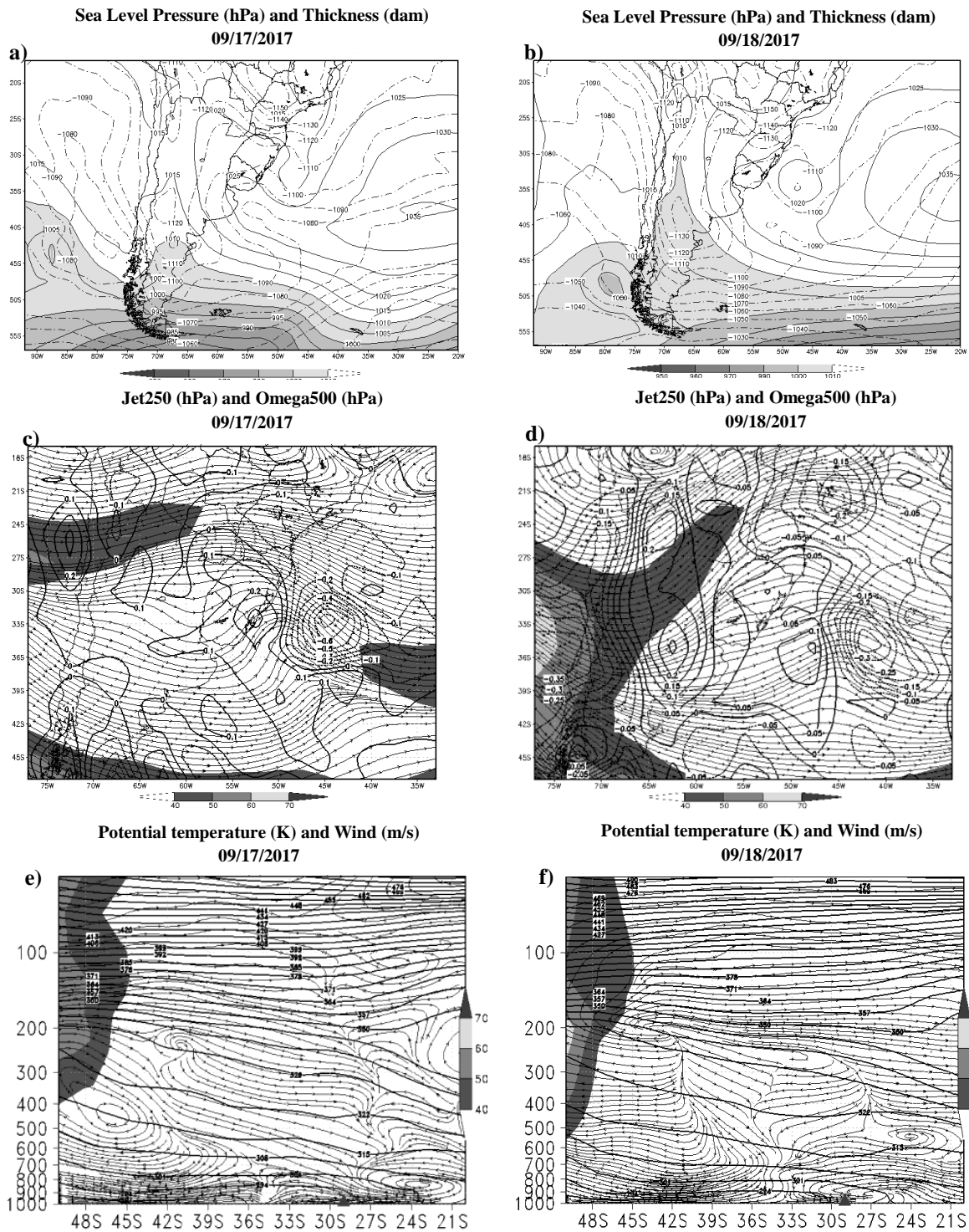
Figure 3: Pressure fields at medium sea level, horizontal cut of the atmosphere and vertical cut between 1000 and 50hPa for days a), c) and e) 09/17/2017 and b), d) and f) 09/18/2017.The red symbol indicates the location of the SSO site.

605
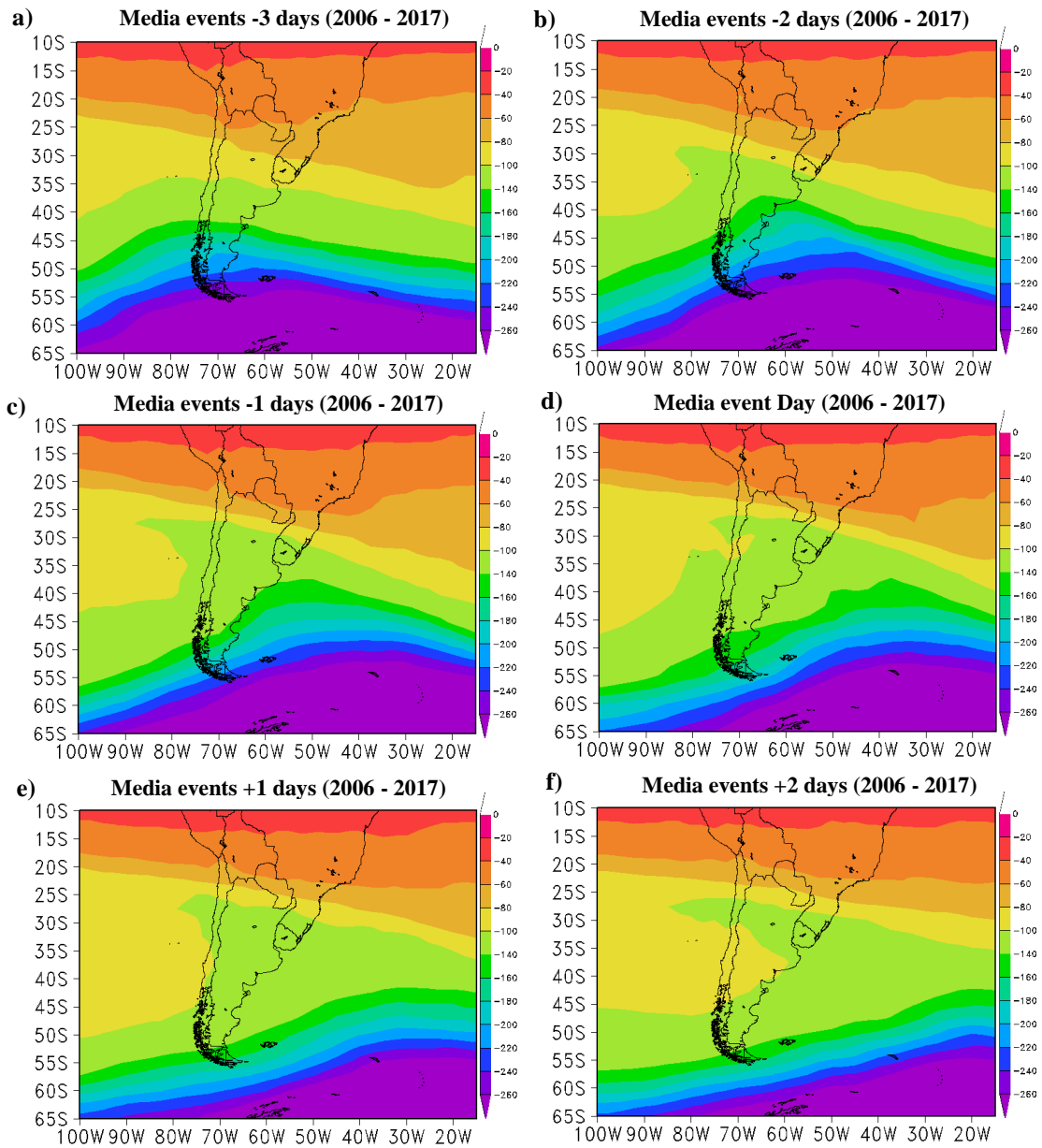
Figure 4: Average PV maps at the 700K isentropic level from 37 PV distributions detected as secondary effect events of AOH: a) -3 days, b) -2 days, c) -1 day, d) day of the event, e) +1 day, f) +2 days.
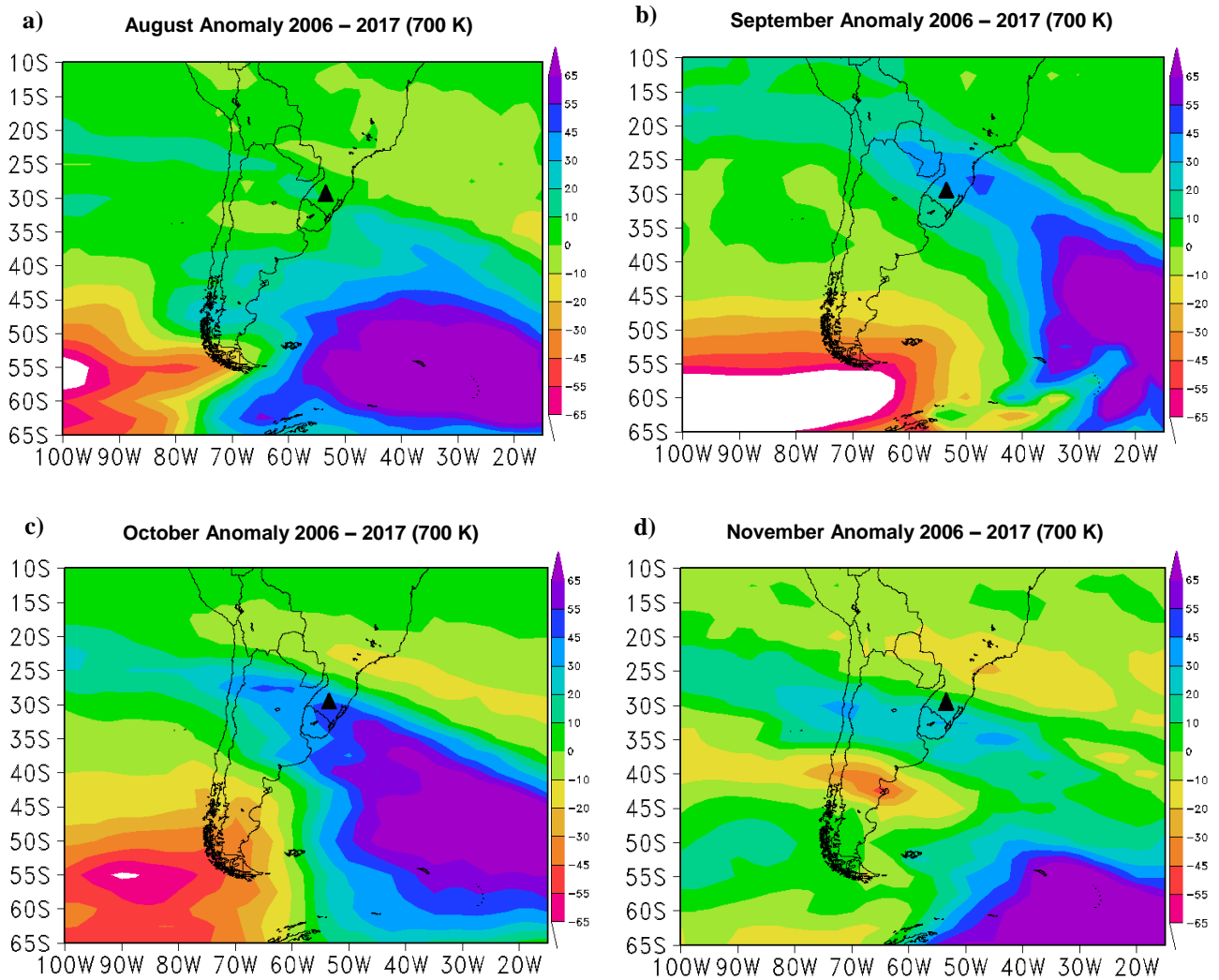
Figure 5: Monthly PV anomaly fields for the period from 2006 to 2017, at the isentropic level of 700 K potential temperature.
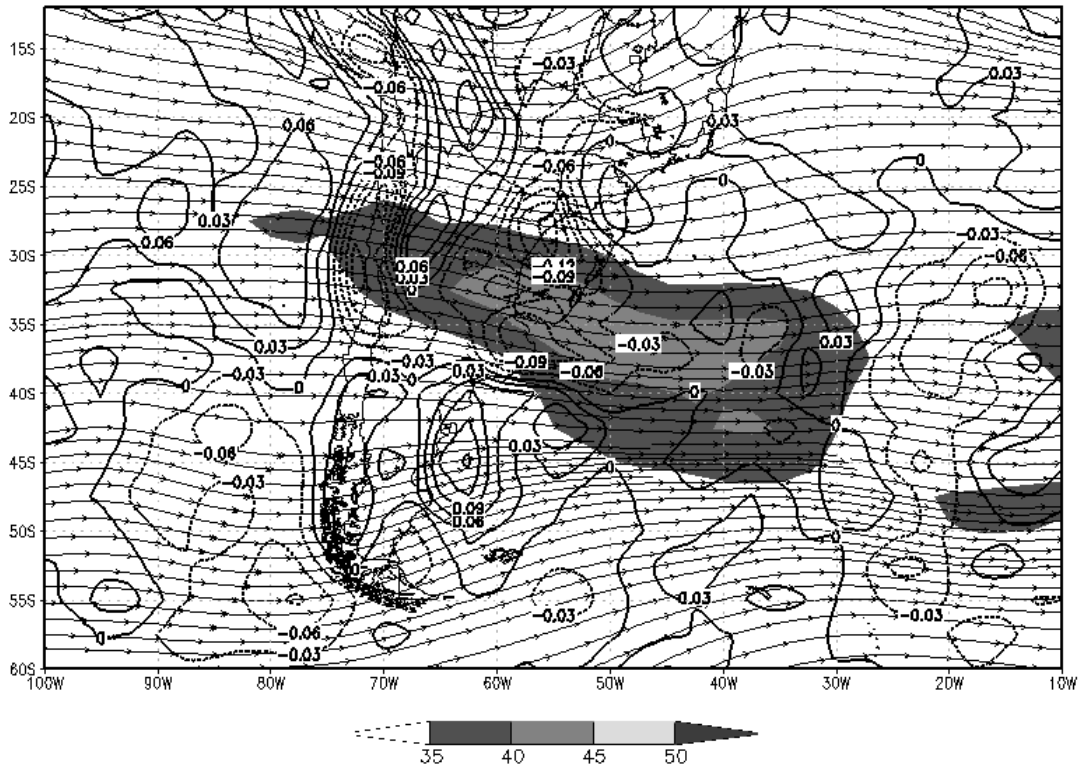
Figure 6: Mean field for the 37 AOH side effect events in the analysis period with jet at 250 hPa (shaded) and Omega at 500 hPa (Omega positive solid lines, Omega negative dotted lines).

660

665
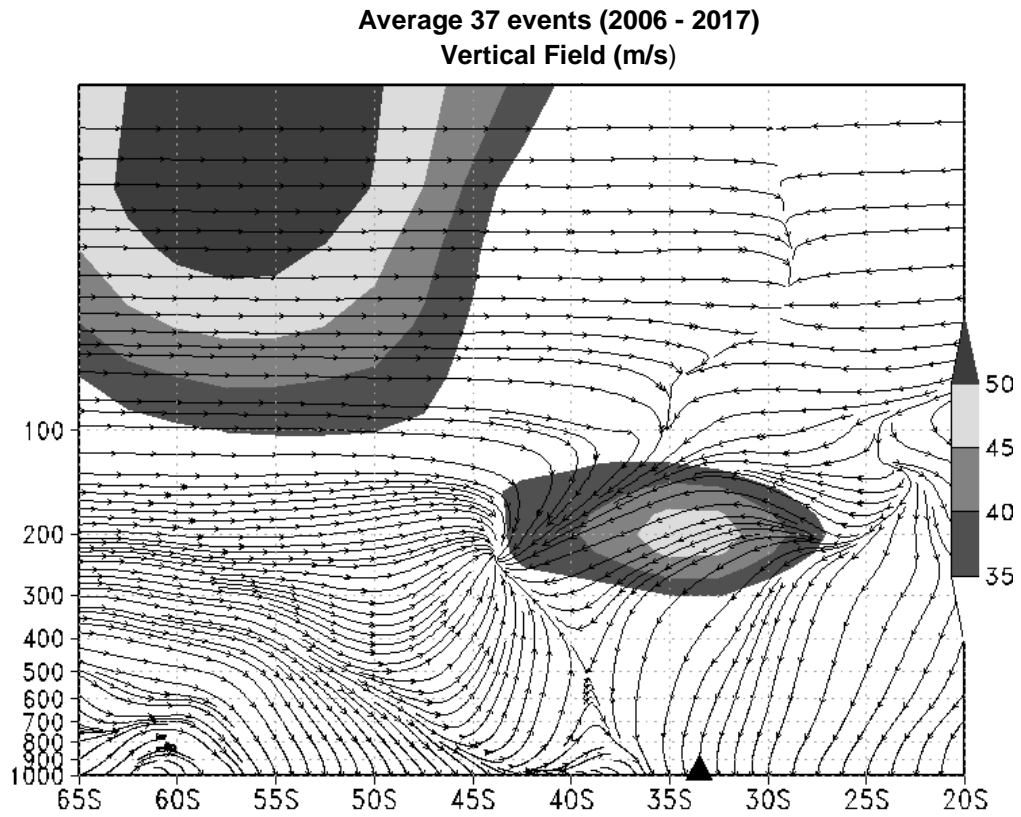
Figure 7: Average for the 37 events of the vertical field between 1000 and 30 hPa, showing the jet current (shaded gray) in
m/s.